Creation efficiency of nitrogen-vacancy centres in diamond

To cite this article: S Pezzagna *et al* 2010 *New J. Phys.* **12** 065017

View the article online for updates and enhancements.

Creation efficiency of nitrogen-vacancy centres in diamond

S Pezzagna[1,2,4]**, B Naydenov**[3]**, F Jelezko**[3]**, J Wrachtrup**[3] **and J Meijer**[1]

[1] RUBION, Ruhr-Universität Bochum, Universitätsstrasse 150, 44780 Bochum, Germany
[2] Research Department IS³/HTM, Ruhr-University Bochum, 44780 Bochum, Germany
[3] 3rd Physical Institute, University of Stuttgart, Stuttgart, Germany
E-mail: sebastien.pezzagna@rub.de

Abstract. Nitrogen-vacancy (NV) colour centres in diamond are attracting growing attention due to potential applications in solid-state quantum information processing and magnetometry. Although proof-of-principle experiments have been demonstrated, further development requires the controllable production of defects with a high yield. In this paper, we experimentally show that the production efficiency of NV defects strongly depends on the ion implantation energy. This can be explained in terms of the number of vacancies produced per implanted ion and surface proximity. The dependence on ion fluence is also underlined, revealing a nonlinear regime and showing how the diamond lattice is damaged at higher fluences.

Quantum computers based on solid state quantum bits (qubits) attracted the attention of many research groups in the last decade [1, 2] because they promise good possibilities for scale-up. Tools to manipulate and implant single atoms, clusters or molecules with nanometer resolution have been successfully developed [3]–[7]. Today, colour centres in diamond and more particularly the nitrogen-vacancy (NV) centre are one of the most promising systems as they fulfil most of the requirements for solid-state qubits (the so-called Di Vincenzo criteria) [8]–[10]. Whether or not scalable quantum computers based on NV can be created

---

[4] Author to whom any correspondence should be addressed.

remains a major question directly related to the creation efficiency of single NV centres. These colour centres possess a strong optical transition from the triplet ground state to the triplet excited state. It has been demonstrated that the electron spin of a single NV centre can be coherently manipulated and optically read out at room temperature [11]–[13]. Moreover, it has been shown that the electron spin coherence time can reach 2 ms [13] in specially grown diamond crystals by using nuclear spin free carbon sources (^{12}C) and by removing other paramagnetic impurities. Recently, the potential of application of single NV centres has been extended to ultrasensitive, nanoscale magnetic field sensors [14]–[16].

In most of the reported experiments, the NV centres were created during the diamond growth. For scalable quantum computer architecture and for magnetometry applications, one needs an accurate positioning of the NV centres as well as a high probability of creation. These two conditions have not yet been simultaneously fulfilled. On the one hand, high yield for NV centres creation (the ratio between active NV centres and the number of implanted N atoms) has already been demonstrated to be up to 50% for high-energy (2 MeV) implantation of nitrogen ions [17], but with an intrinsic straggling of several tens of nanometers. On the other hand, only low-energy implantation (a few keV) can ensure a spatial resolution in the nm range but with much lower yield. For example, Rabeau *et al* [18] reported a 2.5% yield of single NV centres. Usually after implantation, the samples are annealed at high temperature in vacuum in order to induce diffusion of the vacancies, which can then be trapped by the implanted nitrogen atoms [19, 20]. The yield could also be influenced by other factors, such as the background doping or impurity level [21], and, in the case of shallow implanted N, by the proximity to the surface where the vacancies can disappear.

Here, we report on the creation efficiency of NV centres in diamond by direct implantation of nitrogen ions. A large range of energies has been used (between 1.5 keV and 18 MeV) in order to give a complete picture of how the yield of NV creation depends on the ion energy. The samples were characterized using a home-built confocal microscope. The influence of the ion fluence on the NV creation efficiency was also studied and will be discussed below. The idea behind these experiments is to obtain a better understanding of the NV centres formation and how to find conditions to improve their production yield.

Before the implantation, the samples are cleaned in an ultrasonic bath of warm solvent (acetone followed by methanol). After the implantation, the diamonds are annealed for 2 hours at 800 °C in vacuum (pressure 10^{-7} mbar). Then the samples are cleaned in a boiling acid mixture (nitric acid/sulfuric acid/perchloric acid, 1 : 1 : 1) in order to remove graphitic residues and other contaminations from the surface. The implantations in the MeV range are performed in the 4 MV Dynamitron-Tandem accelerator at the University of Bochum. The ion beam can be focused down to diameters $\leqslant 1\,\mu$m by using a superconducting lens [22]. For the implantations in the keV range, a focused ion gun with a gas source is used in a vacuum chamber (10^{-7} mbar). Either molecular or atomic species can easily be selected using a mass filter. The ion beam is focused by a single electrostatic lens, and the beam diameter (between 10 and 40 μm) is measured on a test sample covered with photoresist (PMMA), which changes its colour under ion impact. This effect is directly observed with an *in situ* optical microscope. Finally, the ion current is measured both with a Faraday cup having 0.01 pA precision and with an electron multiplier (in ion counting mode) placed after a 1 μm aperture.

In a first experiment, ^{15}N$^+$ and ^{15}N$_2^+$ stripes are implanted at acceleration voltages of 3, 4 and 5 kV. Figure 1(a) shows a map of fluorescence intensity from the created NV$^-$ centres (band-pass optical filters were tuned for selective detection of negatively charged NV defects). It can
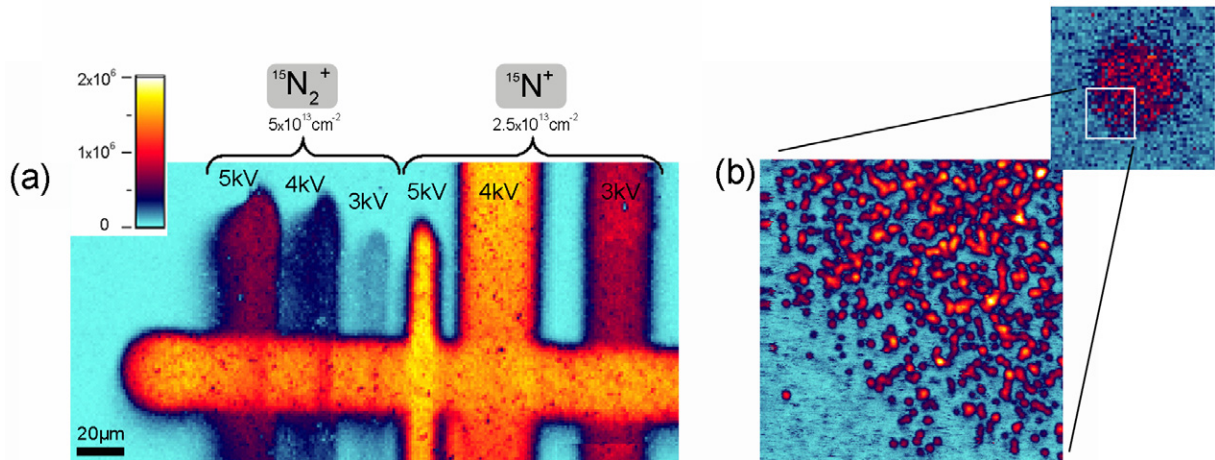
Figure 1. (a) Fluorescence image of an area of a diamond sample presenting vertical stripes implanted with different nitrogen ions (atoms or molecules) and at different acceleration voltages. The narrow lines were implanted using a $10\,\mu$m aperture and the wide lines using a $30\,\mu$m aperture. The colour scale gives the recorded photon counts per second. The horizontal line was implanted as a position reference. (b) $15 \times 15\,\mu$m^2 zoom scan in a focused spot implanted with $5\,$keV ^{15}N$^+$ ions (diameter $25\,\mu$m, fluence of 5×10^{10} cm^{-2}). The density of NV is estimated around $4\,$NVμm^{-2} in the centre. Outside this spot, almost no NV is present, illustrating the high purity of the diamond sample.

be directly seen that, even within these relatively small energy differences, the fluorescence intensity increases significantly with the ion energy, for both the atomic and the molecular ions. Moreover, all the ^{15}N$^+$ stripes are brighter than the ^{15}N$_2^+$ stripes, which have nevertheless been implanted with a higher nitrogen atom density than the ^{15}N$^+$ ones (5×10^{13} cm^{-2} and 2.5×10^{13} cm^{-2}, respectively). Similar implantations have been repeated with a lower and equal fluence of 5×10^{12} nitrogen atoms per cm^2. Again, the same behaviour is observed. For such experiments, the yield Y is given by the following equation:

$$Y = \frac{I_{\text{stripe}}}{I_{\text{NV}}} \cdot \frac{1}{F}, \tag{1}$$

where I_{stripe} is the averaged fluorescence intensity (counts/s and per unit area) of each stripe from which the background fluorescence level has been subtracted, I_{NV} is the fluorescence intensity of a single NV at the same excitation power (calibrated by measuring a saturation curve), and F is the ion fluence. A yield of 0.75% is found for ^{15}N$^+$ ions at $5\,$keV and fluence of 5×10^{12} cm^{-2}.

In the case of lower fluences, one has the possibility of counting directly the number of NV per unit area. This is illustrated in figure 1(b). A $5\,$keV ^{15}N$^+$ focused beam ($25\,\mu$m diameter) is used to implant a fluence of 5×10^{10} ions cm^{-2}. Single NV centres can be seen in the $15 \times 15\,\mu$m^2 zoom and an average density of $4\,$NV$\,\mu$m^{-2} can be determined at the centre of the implanted spot. This gives a yield of 0.8%. Note that such a density corresponds to the superior limit of what is measurable by this technique, as regards the size of a confocal spot $\sim$250–300 nm.

For MeV implantations, patterns such as the one shown in figure 2(a) are implanted with a beam focused below $1\,\mu$m. The created NVs cannot be resolved within a confocal spot.
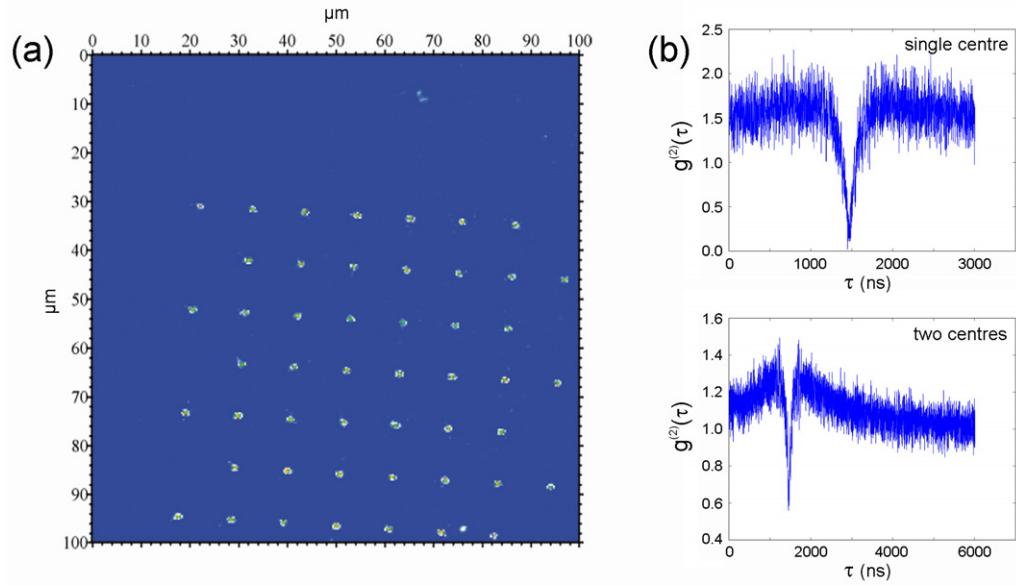
Figure 2. (a) Fluorescence image of an NV pattern implanted by 2 MeV nitrogen ions. (b) Second-order auto-correlation function measurement showing a single (top) and a double (bottom) NV centre. The dip in both graphs occurs at zero time delay.

Nevertheless, if the spots contain only a few NV centres, it is still possible to determine their number by measuring the emitted photon statistics. A single two-level system cannot emit two photons at the same instant and one can determine the number of emitters in a confocal spot by measuring the second-order auto-correlation function:

$$g^{(2)}(\tau) = \frac{\langle I(t) I(t+\tau) \rangle}{\langle I(t) \rangle^2},$$

where the fluorescence intensities at time t and $t + \tau$ are denoted by $I(t)$ and $I(t + \tau)$, respectively. Figure 2 shows $g^{(2)}$ for a single and a double NV, where at zero delay ($\tau = 0$) a dip is observed (anti-bunching) dropping to zero (figure 2(b), top, single NV) or one half (figure 2(b), bottom, double NV). By performing this experiment for all implanted NVs, one could precisely determine the creation efficiency.

In figure 3(a), the yield of NV creation as a function of the ion energy is plotted. The points corresponding to 1.5, 2, and 2.5 keV were measured by using $^{15}N_2^+$ molecular ions having the energy of 3, 4 and 5 keV, respectively. All other points were determined by implanting $^{15}N^+$. It is assumed that when a $^{15}N_2^+$ ion hits the diamond surface, it splits into two atoms having half of the initial energy. Figure 3(a) shows that the creation efficiency of NV centres increases continuously with increasing the ion energy. The slope is strong in the keV region and it becomes smoother at MeV energies. A high yield of 45% is reached at 18 MeV, while for energies lower than 5 keV it is under 1%. As already mentioned, the implantation of low energy ions (<10 keV) is desirable for improving the positioning of the NV. Indeed, the ion straggling is in the range of a few nanometers only for such low energies, as shown in figure 3(c) (SRIM calculation [23]).
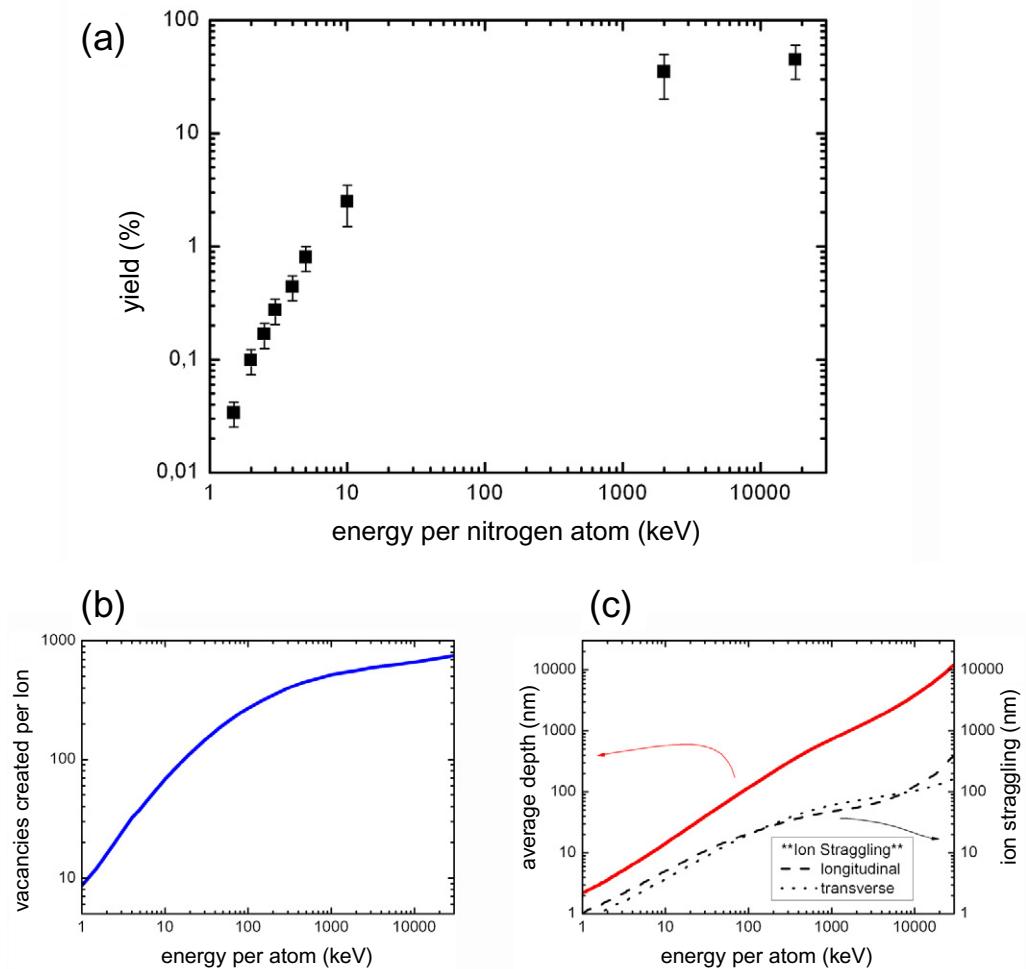
Figure 3. (a) Plot of the measured yield for NV centre creation as a function of the energy per nitrogen atom. (b) Number of vacancies created per implanted $^{15}N^+$ ion as a function of the ion energy (simulated with SRIM). (c) On the left axis: average depth of the implanted $^{15}N^+$ ions as a function of the ion energy. Right axis: longitudinal and transverse ion stragglings as a function of the ion energy (simulated with SRIM).

It is well known that every implanted ion induces along its path in the crystal a certain number of vacancies. The probability of obtaining an NV centre from an implanted nitrogen atom is thus expected to increase with the amount of available vacancies (as long as the crystal lattice is not too damaged). Using SRIM simulations [23], one can estimate the number of vacancies and their distribution along the implantation axis. Figure 3(b) shows the number of created vacancies per ion as a function of the ion energy. The higher the energy, the more vacancies are created around the substitutional nitrogen atom, giving rise to a higher yield as shown by the experimental data in figure 3(a).

Moreover, the curve in figure 3(b) shows a similar behaviour, namely a strong slope at low energy, which becomes smoother at high energy. The yield and number of vacancies appear to be well correlated. Furthermore, if the two curves are superimposed, they start to diverge for energies lower than 10 keV. Note that, in this case, the nitrogen atoms and their surrounding
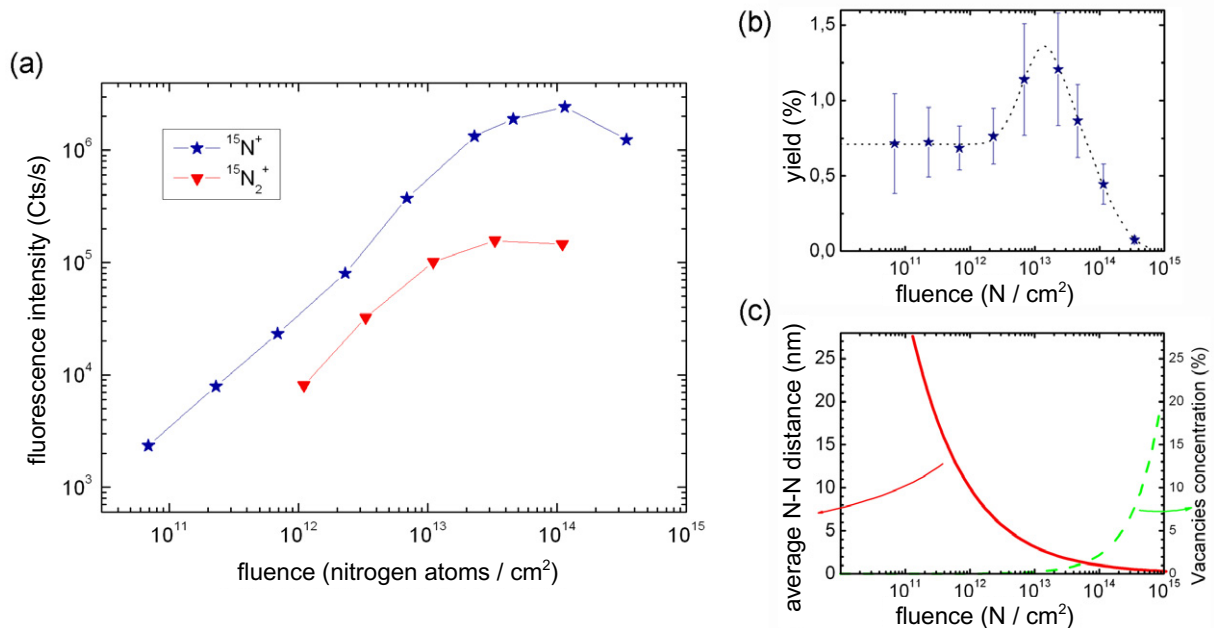
Figure 4. (a) Fluorescence intensity versus fluence for atomic and molecular ions accelerated at 5 kV. The fluence is the number of nitrogen atoms implanted per cm^2, i.e. a $^{15}N_2^+$ ion gives two atoms. (b) Yield versus ion fluence for atomic ions at 5 keV. The dotted curve is a guide for the eye. (c) Red: average in-plane distance between implanted N atoms as a function of the ion fluence. Green: vacancy volume concentration with respect to the carbon atoms in the 10 nm layer under the surface. At 5 keV, the implanted nitrogen atoms have an average depth of 8 nm with a 2 nm straggling, and all the vacancies are produced within 10 nm depth.

vacancy clouds are very close to the surface. This can be seen in figure 3(c). For example, the mean depth of a $^{15}N^+$ ion implanted at 5 keV is approximately 8 nm and most of the vacancies are distributed between the surface and the nitrogen atom. The proximity of the surface is likely to explain the drop in the yield towards low energy as the few vacancies created can easily be destroyed on the surface during the annealing step. Although the diffusion of vacancies is not well understood, this has to be taken into account, especially for such shallow implantations. A possible way of studying this effect would be to overgrow the diamond samples, in order to bury deeper the N atoms. One should also consider the presence of a thin contamination/adsorption layer at the diamond surface, which may also lower the apparent yield for low-energy ions (if some of the latter do not reach the diamond). Nevertheless, simulations show that it can be neglected for energies higher than 1 keV.

The yield strongly depends on the ion energy, mainly through the number of vacancies available to form NV centres. We have also studied the NV creation efficiency as a function of the ion fluence at the energy of 5 keV, of particular interest for the low ion straggling. For this purpose, 15 different areas have been implanted (eight with $^{15}N^+$ and five with $^{15}N_2^+$) with fluence from 6.9×10^{10} cm^{-2} to 3.5×10^{14} cm^{-2}. The yield is determined by measuring the fluorescence intensity of each implanted zone. The results are plotted in figure 4(a), for both the atomic (blue stars) and the molecular (red triangles) species.

IOP Institute of Physics Φ DEUTSCHE PHYSIKALISCHE GESELLSCHAFT

It can be seen that, as expected from figure 3(a), at an equivalent fluence, more NVs are produced in the case of atomic ions. For $^{15}N^+$ ions the fluorescence increases almost linearly with fluence, up to $2 \times 10^{12} \, cm^{-2}$. If the fluence is further increased, the curve bends; then the fluorescence intensity reaches a maximum (at approximately $1.2 \times 10^{14} \, cm^{-2}$) and then starts to decrease. The same behaviour is observed for the $^{15}N_2^+$ ions. This phenomenon illustrates the ion-induced damage of the crystal lattice, which becomes more important and finally leads to the amorphization of the diamond [24]–[26]. We estimate it to occur at about 5×10^{21} vacancies cm^{-3}. This value is comparable with the damage density threshold of 10^{22} vacancies cm^{-3} given by Uzan-Saguy *et al* [24] for diamond. According to them, this threshold does not depend on the energy or the type of ions used. Finally, we calculated the yield of NV for the atomic ions as a function of the fluence (figure 4(b)). For low fluences up to $2 \times 10^{12} \, cm^{-2}$, the yield is constant around 0.7%. Then, surprisingly, it increases, almost doubles, and strongly drops at high fluences exceeding the previously observed amorphization threshold. The fact that in the low implantation regime the yield is independent of fluence indicates that, during the annealing, the vacancies created by one implanted N have no chance of being trapped by another implanted N and form an NV centre with it. Indeed, the increase in the yield starts at $\sim 4 \times 10^{12} \, cm^{-2}$ (i.e. when the average in-plane distance between the implanted N (figure 4(c)) becomes less than 5 nm), when the vacancy clouds around each N start to overlap, resulting in a superior number of vacancies available in the very proximity of each N atom. This positive effect on the yield cannot be further extended since a very high density of the vacancies is reached (as illustrated by the second curve in figure 4(c), showing the vacancy concentration with respect to the carbon atoms), and the diamond structure cannot be recovered during the annealing.

In summary, it has been shown that the yield for NV centres creation increases with the ion energy on the whole studied range from less than 1% to almost 50%. The dependence on the ion fluence also shows that the yield goes up with the number of vacancies available around the implanted N, provided that the amorphization threshold is not reached. These results tend to show that different post-implantation methods can be used to increase the yield by creating more vacancies: carbon implantation, proton or electron irradiation, or even the use of hard x-rays. It would be interesting to explore these methods at high temperatures, keeping the sample under the critical threshold of 5×10^{21} vacancies cm^{-3}. Such experiments could help to determine whether high yields (such as the ones of $\sim 50\%$ obtained for N implantations at MeV energies) can be reached for shallow implanted N, which guarantee low straggling and highly accurate positioning.

Acknowledgments

References

[1] Kane B E 1998 A silicon-based nuclear spin quantum computer *Nature* **393** 133–7
[2] Childress L, Gurudev Dutt M V, Taylor J M, Zibrov A S, Jelezko F, Wrachtrup J, Hemmer P R and Lukin M D 2006 Coherent dynamics of coupled electron and nuclear spin qubits in diamond *Science* **314** 281–5

[3] Meijer J *et al* 2008 Towards the implanting of ions and positioning of nanoparticles with nm spatial resolution *Appl. Phys.* A **91** 567–71

[4] Weiss C D *et al* 2008 Single atom doping for quantum device development in diamond and silicon *J. Vac. Sci. Technol.* B **26** 2596–600

[5] Schnitzler W, Linke N M, Fickler R, Meijer J, Schmidt-Kaler F and Singer K 2009 Deterministic ultracold ion source targeting the Heisenberg limit *Phys. Rev. Lett.* **102** 070501

[6] van der Sar T, Heeres E C, Dmochowski G M, de Lange G, Robledo L, Oosterkamp T H and Hanson R 2009 Nanopositioning of a diamond nanocrystal containing a single NV defect center *Appl. Phys. Lett.* **94** 173104

[7] Schofield S R, Curson N J, Simmons M Y, Rueß F J, Hallam T, Oberbeck L and Clark R G 2003 Atomically precise placement of single dopants in Si *Phys. Rev. Lett.* **91** 136104

[8] Gurudev Dutt M V, Childress L, Jiang L, Togan E, Maze J, Jelezko F, Zibrov A S, Hemmer P R and Lukin M D 2007 Quantum register based on individual electronic and nuclear spin qubits in diamond *Science* **316** 1312–6

[9] Hanson R, Dobrovitski V V, Feiguin A E, Gywat O and Awschalom D D 2008 Coherent dynamics of a single spin interacting with an adjustable spin bath *Science* **320** 352–5

[10] Neumann P, Mizuochi N, Rempp F, Hemmer P, Watanabe H, Yamakasi S, Jacques V, Gaebel T, Jelezko F and Wrachtrup J 2008 Multipartite entanglement among single spins in diamond *Science* **320** 1326–9

[11] Jelezko F and Wrachtrup J 2006 Single defect centres in diamond: a review *Phys. Status Solidi* a **203** 3207–25

[12] Kennedy T A, Colton J S, Butler J E, Linares R C and Doering P J 2003 Long coherence times at 300 K for nitrogen-vacancy center spins in diamond grown by chemical vapour deposition *Appl. Phys. Lett.* **83** 4190–2

[13] Balasubramanian G *et al* 2009 Ultralong spin coherence time in isotopically engineered diamond *Nat. Mater.* **8** 383–7

[14] Degen C L 2008 Scanning magnetic field microscope with a diamond single-spin sensor *Appl. Phys. Lett.* **92** 243111

[15] Maze J R 2008 Nanoscale magnetic sensing with an individual electronic spin in diamond *Nature* **455** 644–7

[16] Balasubramanian G *et al* 2008 Nanoscale imaging magnetometry with diamond spins under ambient conditions *Nature* **455** 648–51

[17] Meijer J, Burchard B, Dohman M, Wittmann C, Gaebel T, Popa I, Jelezko F and Wrachtrup J 2005 Generation of single color centers by focused nitrogen implantation *Appl. Phys. Lett.* **87** 261909

[18] Rabeau J R, Reichart P, Tamanyan G, Jamieson D N, Prawer S, Jelezko F, Gaebel T, Popa I, Dohman M and Wrachtrup J 2006 Implantation of labelled single nitrogen vacancy centers in diamond using 15N *Appl. Phys. Lett.* **88** 023113

[19] Allers L, Collins A T and Hiscock J 1998 The annealing of interstitial-related optical centres in type II natural and CVD diamond *Diam. Relat. Mater.* **7** 228–32

[20] Iakoubovskii K and Adriaenssens G J 2001 Trapping of vacancies by defects in diamond *J. Phys.: Condens. Matter* **13** 6015–18

[21] Wotherspoon A, Steeds J W, Catmull B and Butler J 2003 Photoluminescence and positron annihilation measurements of nitrogen doped CVD diamond *Diam. Relat. Mater.* **12** 652–57

[22] Meijer J, Stephan A, Adamczewski J, Röcken H, Weidenmüller U, Bukow H-H and Rolfs C 1999 Microprobe as implanter for semiconductor devices *Nucl. Instrum. Methods* B **158** 39–43

[23] Zeigler J 2008 The stopping range of ions in matter, SRIM-2008, http://srim.org

[24] Uzan-Saguy C, Cytermann C, Brener R, Richter V, Shaanan M and Kalish R 1995 Damage threshold for ion-beam induced graphitization of diamond *Appl. Phys. Lett.* **67** 1194–6

[25] Gippius A A, Khmelnitskiy R A, Dravin V A and Tkachenko S D 1999 Formation and characterization of graphitized layers in ion-implanted diamond *Diam. Relat. Mater.* **8** 1631–4

[26] Waldermann F C *et al* 2007 Creating diamond colour centers for quantum optical applications *Diam. Relat. Mater.* **16** 1887–95